COMPUTATIONAL INVESTIGATION OF ADVANCED HUB FAIRING CONFIGURATIONS TO REDUCE HELICOPTER DRAG

Walid Khier
Institut für Aerodynamik und Strömungstechnik,
Deutsches Zentrum für Luft- und Raumfahrt e.V. (DLR)
Lilienthalplatz 7, 38108 Braunschweig, Germany
email: walid.khier@dlr.de

ABSTRACT

This paper reports research efforts carried out by the DLR within the framework of the European Commission "Clean Sky" Joint Technology Initiative (JTI) to reduce the aerodynamic drag of helicopters via the application of streamlined hub fairings. A number of three-dimensional RANS simulations of the flow past the GRC common platform fuselage using baseline hub and different generic full fairing shapes were carried out with the unstructured finite volume DLR solver TAU. The computations simulated forward flight at Mach number = 0.204 and an angle of attack ranging between -15^o and 15^o. Chimera overlapping grid method was used to transfer the solution between the fuselage and rotor hub grids, while Wilcox's k-ω two-equation model was employed to simulate the effects of turbulence. The results revealed significant contribution of blade attachments and stubs to hub drag. An overall drag reduction of 17-19% could be obtained by proper optimization of the fairing, blade attachments and stubs

1. INTRODUCTION

The continuous growth of helicopters' share in air traffic together with ever-growing environmental awareness placed additional emphasis on their contribution to acoustic and air pollution. Therefore, future helicopters are expected to fulfill demanding requirements, and to comply with more restrictive emission regulations to gain both administrative approval and public acceptance. Since aerodynamic drag is a key factor affecting helicopters' range, performance and fuel consumption, fulfillment of the previously-mentioned constraints necessitates substantial reduction in aerodynamic drag.

Main rotor hub is one of the major contributors to the aerodynamic drag of a helicopter. Roughly one-third of the total drag of a modern conventional helicopter is attributed to the rotor hub. Consequently, reducing the drag of the main rotor hub is an essential step towards the development of efficient, low emission helicopters.

The European Commission 7th Framework Programme for collaborative research has defined therefore the reduction of helicopter aerodynamic drag as one of the main goals of its "Clean Sky" Joint Technology Initiative (JTI), and established a separate platform within JTI under the name Green Rotor Craft (GRC) dedicated to the achievement of this goal.

The unfavorable drag characteristics of rotor hubs are mainly due to their complex design which involves several bulky components. The position of the rotor hub inside the accelerated flow region above, and in its immediate vicinity of the fuselage, are additional factors increasing the drag of the hub.

Owing to the significance of hub drag, a great deal of research efforts has been dedicated over the past five decades to its analysis and reduction relying mostly on experimental investigations of reduced scale models ([1]-[8]). The majority of these investigations indicated that streamlining the main rotor hub and using pylon and mast

fairings are efficient means to reduce the overall drag of the helicopter.

Recent research efforts involved the application of CFD. Wake *et al* examined the capabilities of CFD to predict the drag of hub-mast fairing system of Sikorsky's X2 Technology™ Demonstrator in [12], while others applied CFD to tackle problems related to the rotor hub, like, for example, hub-fuselage interaction ([9]-[11]).

This paper reports CFD analysis performed by DLR within the GRC program to reduce hub drag using streamlined hub fairings. The investigation focuses on the influence of fairing shape on the aerodynamic loads acting on the so-called GRC2 common platform helicopter in cruise flight under different pitch conditions. Section 2 describes the GRC2 common platform configuration and the computational model derived therefrom, while section 3 briefly describes the numerical method; section 4 reports the general characteristics of the grid systems; the numerical results are presented and discussed in section 5. Finally summary of the investigations and the conclusion drawn therefrom are given in the last section: section 6

2. BASELINE AND TESTED CONFIGURATIONS

The GRC2 common platform helicopter model was derived from the 1:3881 th scale GOAHEAD [13] wind tunnel model (Figure 1) by adding sponsons and modifying the position and orientation of the horizontal stabilizer.

The tail rotor blades, hub, gearbox and all its other mechanical components were not considered in all computations reported here.

In an attempt to investigate the aerodynamic interference between the hub and fuselage, the engine cowl and shaft fairing were blended together to reduce the acceleration of the flow over top of the helicopter. Figure 3 compares the hereinafter designated "modified fuselage" with the baseline fuselage.

All of the major components of a typical rotor head were simplified by removing tiny details, like hardware, cables, connectors, etc., and by reducing the geometry of the components to simple shapes. Detailed description of the original model and the geometrical modifications introduced are given in [14].

As for the hub fairing, two shapes are examined and judged against the baseline hub. The first, designated FF-V3 has a flat base and reflex curvature upper surface. FF-V3 shares the same blade stubs with the baseline hub, but the fairing partially covers the blade attachments. The second fairing, designated FF-V5, features streamlined blade stubs blended in the fairing's surface [15]. This resulted in a raised belt line to match the leading and trailing edges of the stubs. Therefore, a flat underside was no longer possible to maintain. Figure 4 illustrates the different fairing shapes and compares their cross sections with the baseline hub.

Four configurations were tested: the baseline fuselage+baseline hub, modified fuselage+FF-V3, baseline fuselage+FF-V3, and baseline fuselage+FF-V5.

For the first two configurations (baseline configuration and modified fuselage+FF-V3) the pitch angle was swept between α=-15^o to α=15^o, while in the other two, baseline fuselage+FF-V3, and baseline fuselage+FF-V5 the pitch angle variation was limited between α=-5^o to α=5^o.

3. NUMERICAL APPROACH

The numerical approach employed in this paper is based on the solution of the stationary Reynolds (Favre) averaged Navier-Stokes equations in three dimensions by means of the DLR CFD unstructured simulation code TAU [15]. The solver relies on cell vertex scheme to discretize the mass, momentum and energy fluxes, which are represented by either central scheme or a variety of upwind schemes of second-order accuracy. Third order numerical dissipation is added to the convective fluxes to ensure numerical stability. The dissipative fluxes are computed using either scalar or matrix formulation. The solver also features Low Mach number preconditioning to extend the application of the code to the incompressible regimes. Multi-stage Runge-Kutta explicit or implicit LU-SGS time integration schemes are used to advance the solution in artificial time in the case of steady simulation, and dual-time approach is employed for time accurate simulations. TAU allows rotors and propellers to

be presented by an actuator disc following the original Froude actuator disc model but with modifications to handle compressibility effects [17]. Chimera technique [16]-[17] is available to facilitate grid generation task and to perform simulations involving relative body motion. A wide array of statistic turbulence models, ranging from algebraic, one- and two-equation eddy viscosity models ([18]-[20]) to seven-equation Reynolds stress model ([21]-[23]) is available in TAU to simulate the effects of turbulence. In this paper multi-stage Runge-Kutta is used to represent the inviscid fluxes with scalar artificial dissipation. Turbulence effects are accounted for by the two-equation Wilcox's k-ω model.

4. NUMERICAL GRID

CENTAUR® was used to generate separate grids around the rotor hub and the fuselage. These component grids were later combined by Chimera to compose the numerical grid (Figure 5). Table 1 and Table 2 respectively summarize the characteristics of the fuselage and hub grids.

Nr. of	BL Fuselage	Mod. Fuselage
points	7 328 773	7 227 849
tetrahedrals	25 455 728	24 647 497
prisms	5 475 265	5 643 478
pyramids	113 163	98 086

Table 1: Baseline and modified fuselage grid parameters

Nr. of	BL Hub	FF-V3	FF-V5
points	23 001 794	5 877 606	7 649 654
tetrahedrals	32 176 132	24 815 932	31 302 744
prisms	33 805 292	2 845 816	4 197 172
pyramids	148 092	46 848	62 532

Table 2: Baseline and streamlined fairings grids.

5. RESULTS

Figure 8 presents the drag and lift of the fuselage for the four configurations as a function of the pitch angle α. From the figure it can be seen that the drag of the modified fuselage exceeds baseline fuselage above $\alpha = -5^o$, but improves the lift up to α values almost equal to 2^o. The baseline fuselage performs slightly better than the modified fuselage when both are combined with full fairing FF-V3 showing lower drag, however, its lift is slightly less than the modified fuselage. An evident reduction in fuselage drag due to the full fairing FF-V5 can be clearly seen. The drag of the baseline fuselage drops by almost 8% at $\alpha = -5^o$, and at the same time, the lift increases by 12%. This gain in drag vanishes with increasing the pitch angle reaching nearly 0.5% at $\alpha = 5^o$. The lift behaves almost linearly with the pitch angle but at a lower gradient compared to the baseline configuration. This trend is reversed above $\alpha = 0^o$, where the lift falls below the value of the baseline case.

Hub drag and lift variation with the pitch angle are shown in Figure 7. Examination of the figure shows that the shape of the fuselage has a trivial effect on the drag of the full fairing FF-V3. Except for pitch attitudes as low as $\alpha = -8^o$, FF-V3+modified fuselage has broadly better drag characteristics than the baseline hub+baseline fuselage. In view of the negligible influence of the fuselage pointed out earlier, it is safe to assume that drag improvements would be sustained if the baseline fuselage is used in this range of α. The advantages of full fairing increase with the pitch angle beyond $\alpha = -8^o$ reaching 31% at $\alpha = 5^o$, then remain almost constant up to $\alpha = 15^o$. FF-V5 has significantly lower drag than the baseline hub. The gain in drag ranges between 34% and 47% at $\alpha = -5^o$, and 5^o respectively. Regardless of the fuselage used, all hub shapes examined show almost linear lift with pitch altitudes. The lift of FF-V3 coincides with the baseline hub at $\alpha=0^o$, but changes with α at a greater rate leading to gain in lift for nose up positions and a loss in lift in the nose down positions. The modified fuselage reduces FF-V3 lift, but does not change its gradient. Therefore, the lift of FF-V3 remains lower than the lift of baseline hub for higher values of α when the modified fuselage is used than

when the baseline is combined with FF-V3. Considerable increase in lift is observed for FF-V5 reaching roughly 300% of the baseline hub lift at $\alpha=5^o$.

Finally, the total forces are compared in Figure 8. The figure indicates a reduction in the overall drag of 3.13 – 4.92% by using full fairing FF-V3 with nearly no loss in lift. As can be seen from the figure, the baseline fuselage + FF-V3 is identical to, if not better than, the combination of modified fuselage + FF-V3. Obviously FF-V5 is superior to the other two fairing shapes where remarkable gain in the overall drag ranging between 17% and 19% could be obtained. The figure also indicates that the overall lift is improved only by using FF-V5. As for the other configurations, no significant variation in overall lift could be detected except some modest variation in strong pitch conditions below $\alpha=-5^o$ and above $\alpha=5^o$.

Hub drag breakdown given in Figure 9 for the three hub shapes explains how the full fairing reduces the drag. In the original design, 70% of the drag is caused by the blade stubs and attachments, with a contribution of the stubs between 40% and 50% of the drag. Small components like the dampers have a share of less than 4.5% of hub drag. The remaining 25.5% is divided almost equally between the beany (denoted hub in the figure) and the shaft. In the case of FF-V3 fairing, the dampers are enclosed inside the fairing, and consequently, their effect is eliminated. However, what the fairing essentially does is to isolate the blade attachments, thus causing the fairing surface (denoted hub in the figure) and the blade stubs to dominate the drag breakdown with 46% to 48%, and 46%-47% of hub drag attributed to the fairing surface and blade stubs respectively. Streamlining and blending the stubs with the surface of the fairing in FF-V5 reduces hub drag significantly as indicated earlier, but does not affect the breakdown pattern much. The figure shows that 43% to 45% of the hub drag is due to the blade stubs.

The drag polar plots depicted in Figure 10 reveal that the full fairing FF-V3 drag is about 38% less than the baseline for the same lift at the extrema, and 30% at the baseline hub minimum drag point. The corresponding values for FF-V5 are 56% and 32%, respectively, and 29% at FF-V5 maximum drag point. As far as the total drag is concerned, FF-V5 results show a remarkable drag saving of 22.5% and 12.3% at the extrema, and 20% at the baseline minimum drag point.

6. CONCLUSIONS

A series of numerical investigations has been carried out to analyze and reduce the aerodynamic helicopter drag. The study was particularly aimed at the optimization of the GRC common platform helicopter drag by the application of full fairings to reduce the parasitic drag of the main rotor hub. Two full fairing shapes, denoted FF-V3 and FF-V5, were designed and their performance was analyzed. In addition, an attempt was made to reduce the interference drag by modifying the engine and shaft fairing of the fuselage. Analysis and evaluation of the results revealed the following:

- The drag breakdown of the baseline hub is dominated by blade attachments and stubs, whose contribution is around 70% of the hub drag, which constitutes roughly 20% of the overall drag of the helicopter.

- Therefore, efficient reduction of drag must include treatment of the bluff blade stubs and attachments. The current study has shown that covering the attachments leads to 3.13 – 4.92% reduction in the total drag, while streamlining the bluff parts of the stubs (together with the associated modification of the fairing) improves this gain to 17 to19%.

- At constant lift conditions, up to 6% reduction in helicopter drag was achieved by streamlining the fairing (FF-V3), and up to 20% by FF-V5 at the minimum drag point of the baseline configuration. The savings at the extreme points of the baseline fuselage+FF-V5 configurations are 12.3% and 22.5%

- The present analysis explored the potential of different fairing basic shapes to reduce the drag. Detailed investigations of the selected configurations under various flight conditions, possibly using advanced optimization techniques, is believed to lead to additional improvements in drag.

- The optimization efforts reported in this paper focused on cruise flight conditions only. Additional investigations under different flight conditions are required to confirm the benefits of full fairing.

- The influence of the new hub design on the dynamics of the aircraft was not studied. Tail shake and other interference phenomena related to rotor hub have yet to be investigated

Acknowledgment

The presented investigation was carried out within the framework of the European Union Green Rotor Craft Integrated Technology Demonstrator (GRC-ITD) under contract number CSJU-GAM-GRC-2008-00. The author would like to acknowledge the European Union for funding this work.

7. REFERENCES

[1] Sheehy, T., et al, A Method for Predicting Helicopter Hub Drag, United Technologies Corporation Report Nr. AD-A021 201, January 1976.

[2] Sheehy, T., A General Review of Helicopter Rotor Hub Drag Data, AHS Meeting, Stratford, December 1975

[3] Strob, R. H., Young, L. A., Graham, D. R., Louie, A. W., Investigation of Generic Hub Fairing and Pylon Shapes to Reduce Hub Drag, NASA Technical Memorandum 100008, September 1987

[4] Graham, D. R., Sung, D. Y., Young, L. A.,Louie, A. W., Stroub, R. H., Helicopter Hub Fairing and Pylon Interference Drag, NASA Technical Memorandum 101052, January 1989

[5] Sung, D. Y., Lance, M. B., Young, L. A., Stroub, R. H., An Experimental Investigation of Rotor Hub Fairing Drag Characteristics, NASA Technical Memorandum 102182, September 1989

[6] Young, L. A., Graham, D. R., Experimental Investigation of Rotorcraft Hub and Shaft Fairing Drag Reduction, AIAA 86-1783.

[7] Young, L. A., Graham, D. R., Strob, R. H., Experimental Investigation of Rotorcraft Hub and Shaft Fairing Drag Reduction, Journal of Aircraft Vol. 24, Nr. 12December 1987.

[8] G. E. Sweet, J. L. Jenkins, Wind Tunnel Investigation of the Drag and Static Stability Characteristics of Four Helicopter Fuselage Models, NASA TN D-1363, July 1962.

[9] Khier, W., Numerical Analysis of Hub and Fuselage Interference to Reduce Helicopter Drag, Proceedings of the 38th European Rotorcraft Forum, Amsterdam, The Netherlands, 4-7 September 2012. ISBN: 9781627480611.

[10] Lee, B. S., Jung, M. S., Kwon, O. J., Kang, J. J., Numerical Simulation of Rotor-Fuselage Aerodynamic Interaction Using an Unstructured Overset Mesh Technique Int'l J. of Aeronautical & Space Sciences, Vol. 11, No. 1, March 2010.

[11] Borie, S.,.Mosca, J., Sudre, L.,. Benoit, C., Péron, S., Influence of rotor wakes on helicopter aerodynamic behavior, 35th European Rotorcraft Forum, Hamburg, Germany, 22-25 September 2009. ISBN: 9781615678747.

[12] Wake, B., E., Hagen, E., Ochs, S., S., Matalanis, C. G., Scott, M., W., Assessment of Helicopter Hub Drag Prediction with an Unstructured Flow Solver. 65th American Helicopter Society Annual Forum, Grapevine, Texas, 27-29 May 2009. Technologies Research Center. Published with permission.

[13] Pahlke, K., The GOAHEAD project, Proceedings of the 33rd European Rotorcraft Forum, Kazan, Russia, September 2007.

[14] D'Alascio, A., Kneisch, T., Desvigne D. Specification of Geometrical Constraints and of the Design Points for Common Helicopter Platform Optimisation Subtasks. GRC Internal Report CSJU/ITD GRC/RP/2.2.2/32024 – Issue 7 (07.05.2014)

[15] Khier, W., Numerical Analysis of Hub and Fuselage Interference to Reduce Helicopter Drag, Bericht des Institutes für Aerodynamik und Strömungstechnik, Deutsches Zentrum für Luft-undRaumfahrt e.V., Lilienthalplatz 7, 38108 Braunschweig, Germany, IB 124-2013/912

[16] Schwamborn, D.; Gerhold, T.; Heinrich R., The DLR Tau-code: Recent Applications in Research and Industry. In: Proceeding of ECCOMAS CFD 2006, Egmond aan Zee, Netherlands, September 5th-8th, 2006.

[17] Raichle, A., Melber-Wilkending, S., Himische, J., A New Actuator Disc Model for the TAU Code and Application to a Sailplane with a Folding Engine, Contributions to the 15th STAB/DGLR Symposium, Darmstadt, Germany, 2006.

[18] Benek, J.A., Steger, J. L., Dougherty, F. C., A flexible grid embedding technique with application to the Euler equations. In 6th Computational Fluid Dynamics Conference, Danvers, MA. AIAA 83-1944,1983.

[19] Madrane, A.; Raichle, A.; Stürmer, A., Parallel Implementation of a Dynamic Overset Unstructured Grid Approach. In: ECCOMAS 2004, Jyväskylä,, Finland, 24.-28. July 2004.

[20] Spalart, P. R., Allmaras, S. R., A One-Equation Turbulence Model forAerodynamic Flows, AIAA 30th Aerospace Sciences Meeting and Exhibit., Reno, NV, USA, 6-9 January, 1992.

[21] Wicox, D., C., Reassessment of the Scale-Determining Equations for Advanced Turbulence Models, AIAA Journal, vol. 26, no. 11, November 1988

[22] Menter, F. R., Two-Equation Eddy-Viscosity Turbulence Models for Engineering Applications, AIAA Journal Vol. 32 No. 8, August 1994.

[23] Launder, B. E., Reece, G. J., Rodi, W., Progress in the Development of a Reynolds-Stress Turbulence Closure, Journal of Fluid Mechanics, 68: 537-566, 1975.

[24] Speziale, C. G., Sarkar, S., Gatski, T. B., Modelling the Pressure-Strain Correlation of Turbulence: An Invariant Dynamical Systems Approach. Journal of Fluid Mechanics, 227, 245-272, 1991.

[25] Eisfeld, B., Brodersen, O., Advanced Turbulence Modelling and Stress Analysis for the DLR-F6 Configuration, 23rd AIAA Applied Aerodynamics Conference, 6-9th June 2005, Toronto, Canada.

Figure 1: The GOAHEAD configuration inside the DNW-LLF wind tunnel

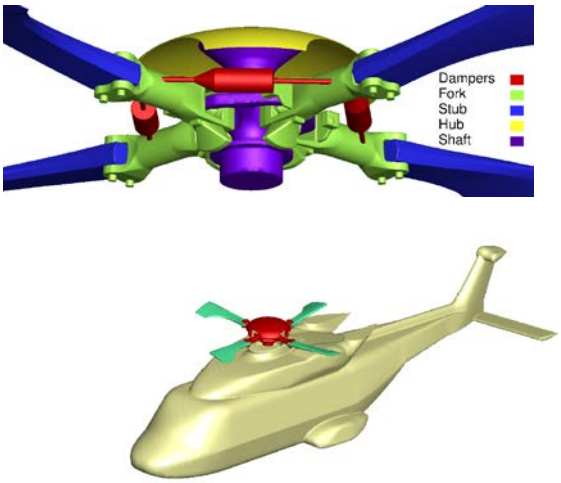

Figure 2: Computational model of the simplified common platform helicopter (left). Right: computational model of the hub showing its main components (excluding push rods)

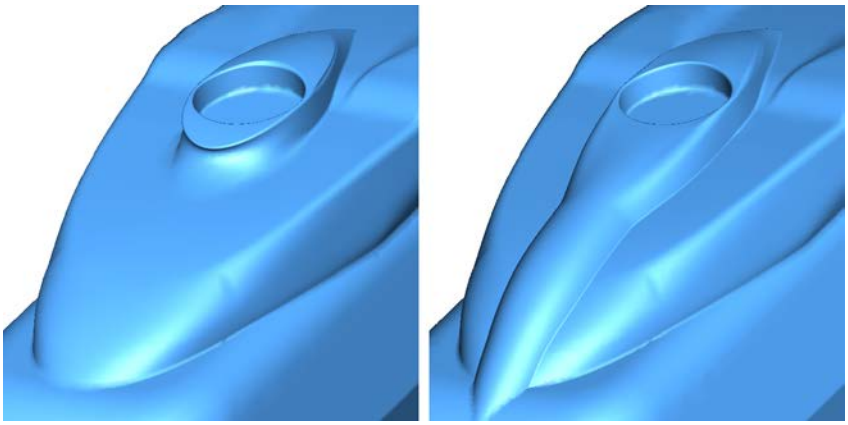

Figure 3: Comparison of baseline fuselage geometry (left) and modified fuselage (right) showing the blending of engine cowl with shaft fairing.

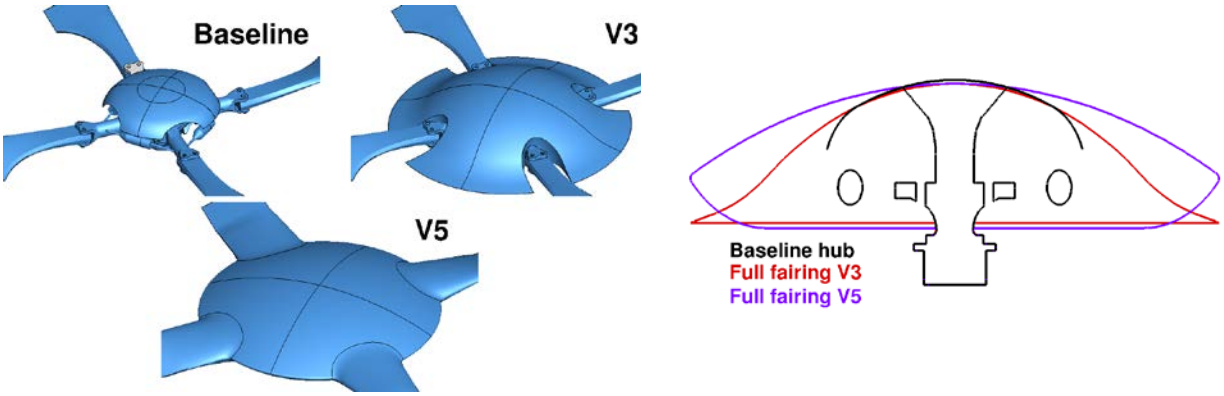

Figure 4: Left: Hub fairing shapes. Right: Hub fairing cross sections

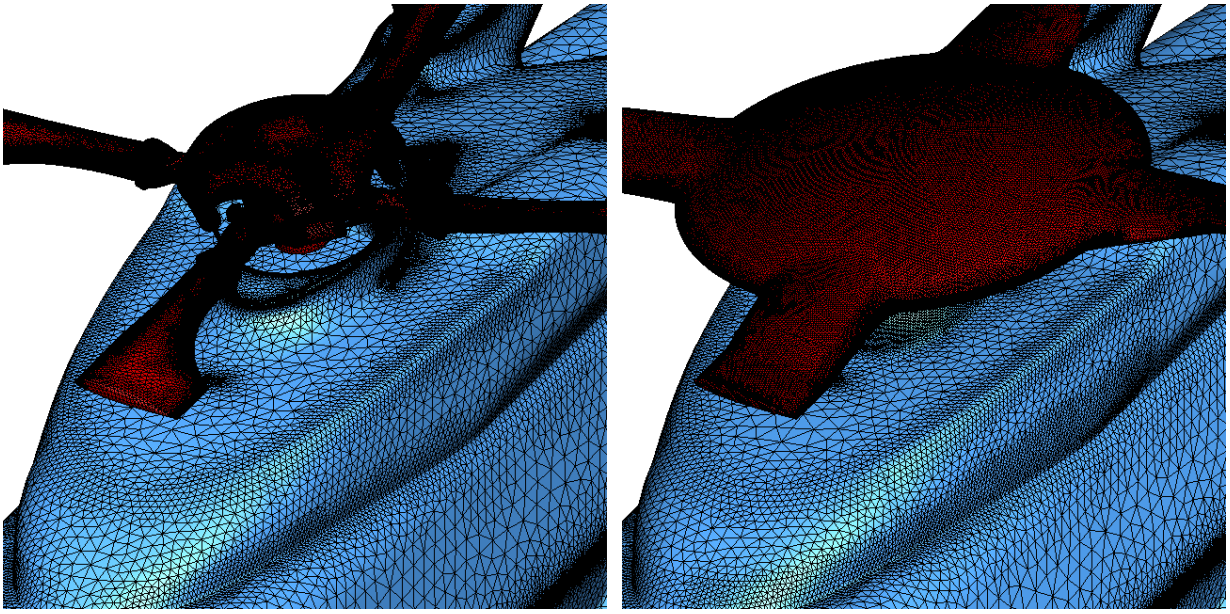

Figure 5: Comparison of surface grids on the baseline configuration (Left) and baseline fuselage + full fairing FF-V5

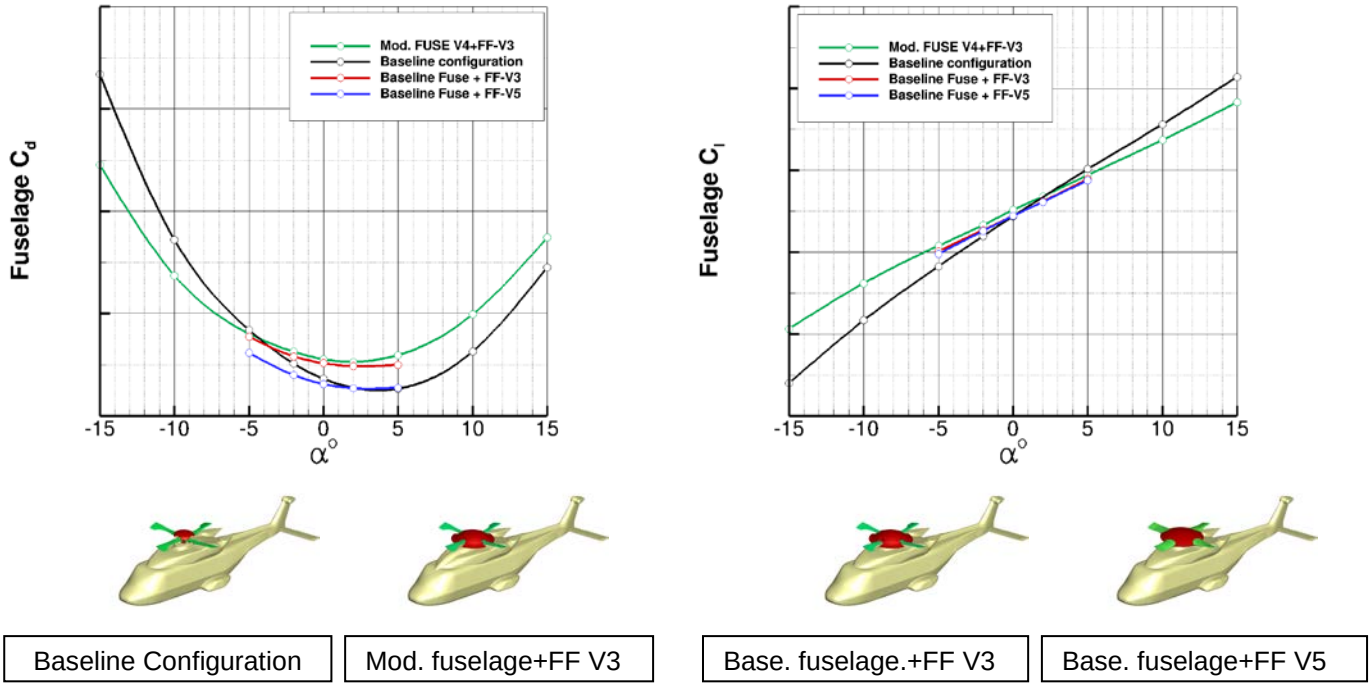

Figure 6: Fuselage drag (left), and lift (right) polars for different configuration in free stream conditions at cruise Mach number Ma=0.204

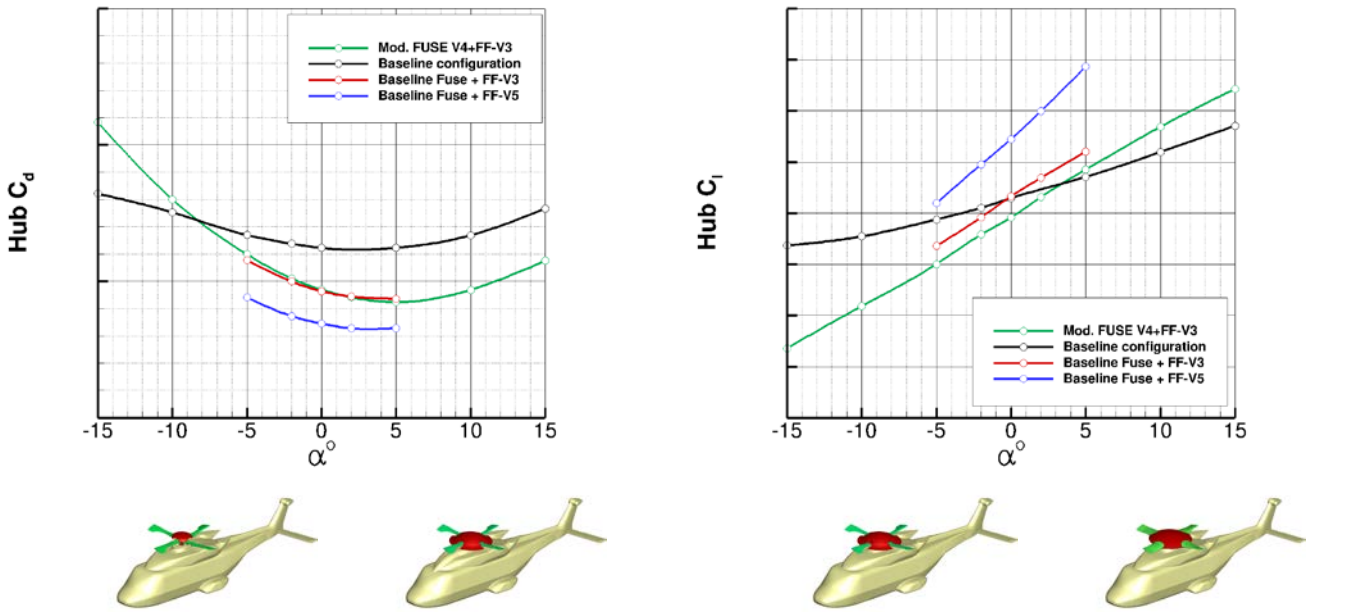

Baseline Configuration	Mod. fuselage+FF V3	Base. fuselage.+FF V3	Base. fuselage+FF V5

Figure 7: Hub drag (left), and lift (right) polars for different configuration in free stream conditions at cruise Mach number Ma=0.204

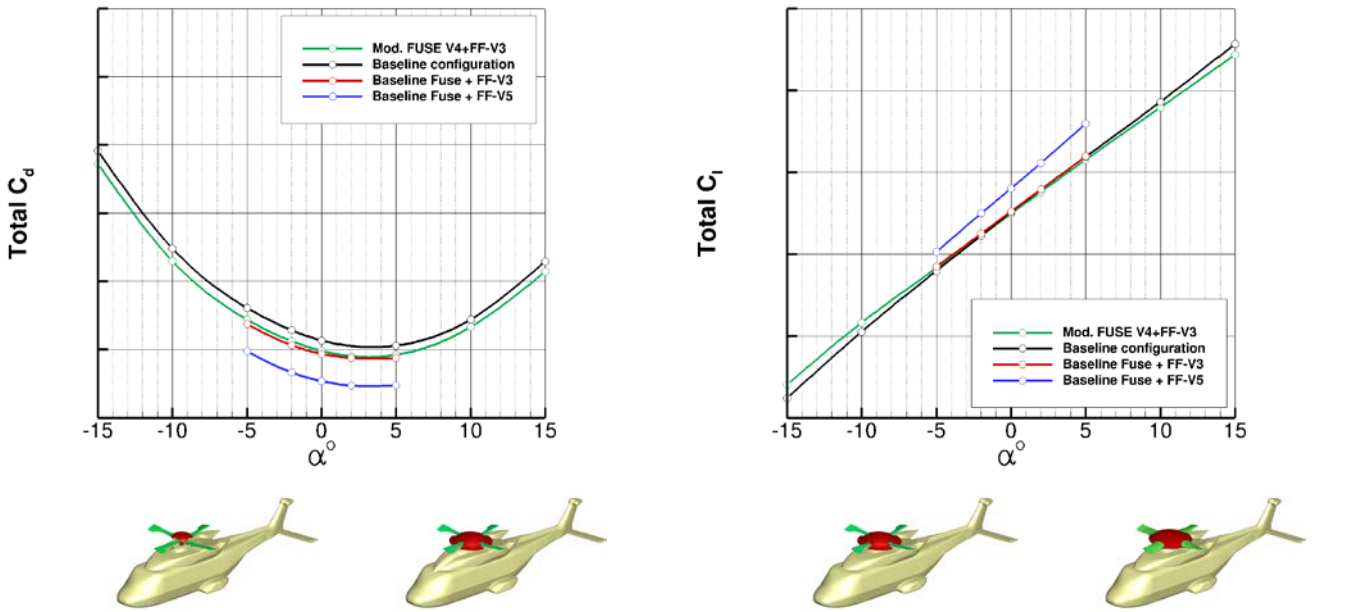

Baseline Configuration	Mod. fuselage+FF V3	Base. fuselage.+FF V3	Base. fuselage+FF V5

Figure 8: Overall drag (left), and lift (right) polars for different configuration in free stream conditions at cruise Mach number Ma=0.204

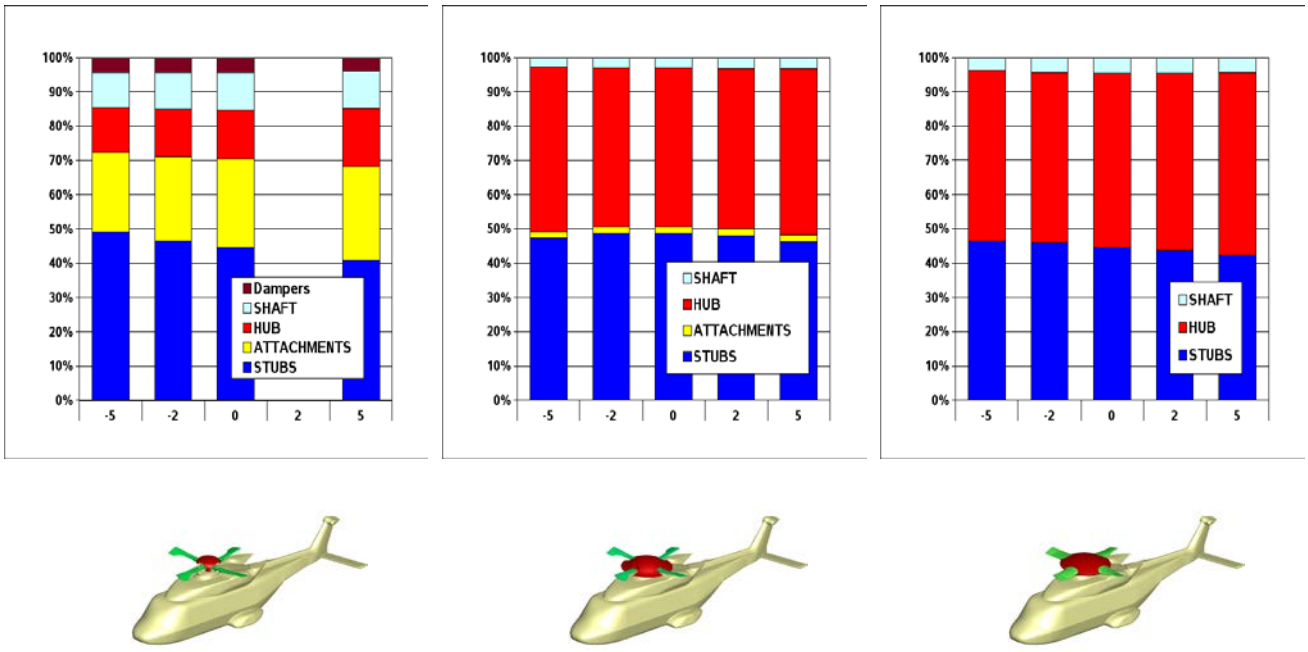

Figure 9: Hub drag breakdown as a function of the pitch angle. Left: Baseline configuration. Center: Baseline fuselage+FF-V3. Right: Baseline fuselage+FF-V5. Note the no data is available for the baseline configuration under -2^{o} pitch angle

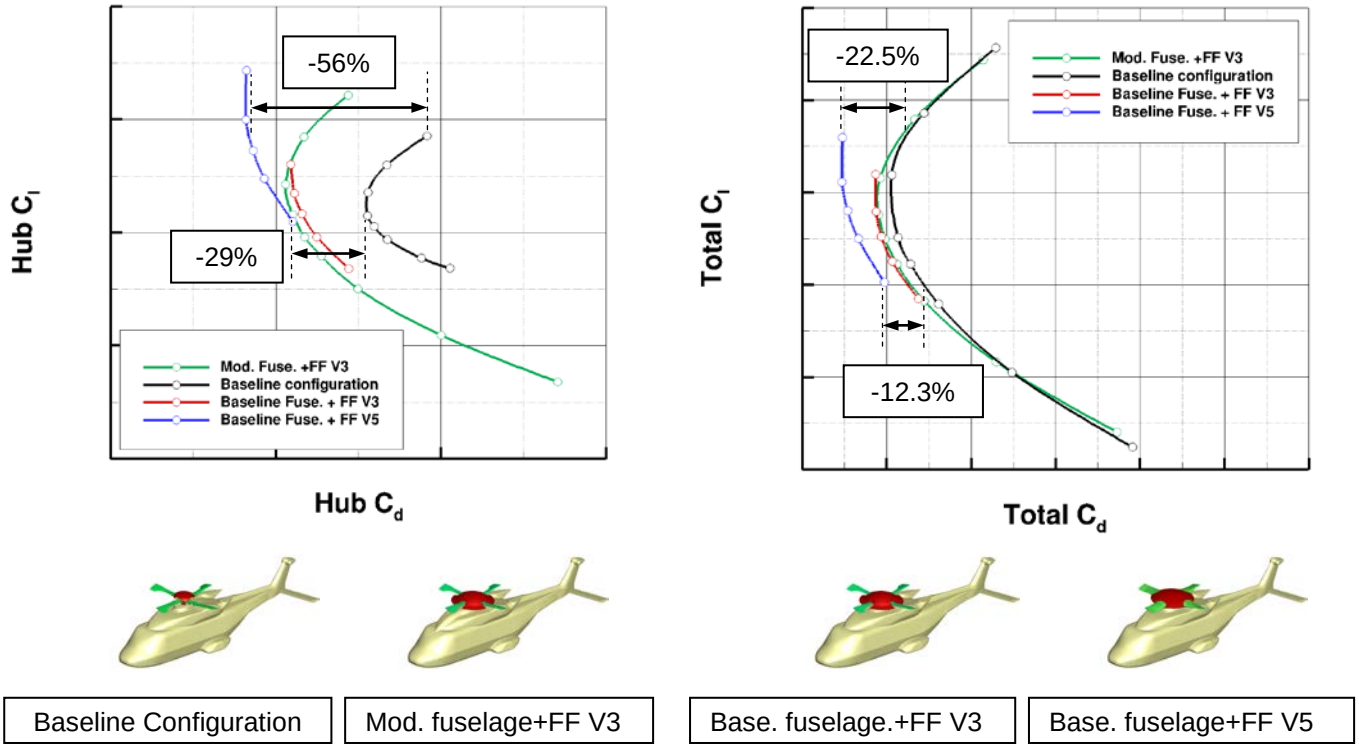

Figure 10: Drag-lift polars for the hub (left), and the complete configuration (right) for different configurations in free stream conditions at cruise Mach number Ma=0.204